IOP Publishing Mater. Res. Express 5 (2018) 036415 https://doi.org/10.1088/2053-1591/aab4a6

Materials Research Express

PAPER

RECEIVED
13 February 2018

REVISED
1 March 2018

ACCEPTED FOR PUBLICATION
7 March 2018

PUBLISHED
28 March 2018

Theoretical and experimental investigation of conjugation of 1,6-hexanedithiol on MoS_2

A Gul[1], C Bacaksiz[2], E Unsal[2], B Akbali[2], A Tomak[3], H M Zareie[4] and H Sahin[5,6]

[1] Department of Bioenginnering, Izmir Institute of Technology, 35430, Izmir, Turkey
[2] Department of Physics, Izmir Institute of Technology, 35430, Izmir, Turkey
[3] Department of Materials Science and Engineering, Izmir Institute of Technology, 35430, Izmir, Turkey
[4] Microstructural Analysis Unit, School of Physics and Advanced Materials, University of Technology, 2007, Sydney, Australia
[5] Department of Photonics, Izmir Institute of Technology, 35430, Izmir, Turkey
[6] ICTP-ECAR Eurasian Center for Advanced Research, Izmir Institute of Technology, 35430, Izmir, Turkey

E-mail: hasansahin@iyte.edu.tr

Keywords: TMDs, first principles, Raman spectroscopy, conjugation of MoS_2, vibrational spectra, HOMO-LUMO

Abstract

We report an experimental and theoretical investigation of conjugation of 1,6-Hexaneditihiol (HDT) on MoS_2 which is prepared by mixing MoS_2 structure and HDT molecules in proper solvent. Raman spectra and the calculated phonon bands reveal that the HDT molecules bind covalently to MoS_2. Surface morphology of MoS_2/HDT structure is changed upon conjugation of HDT on MoS_2 and characterized by using Scanning Electron Microscope (SEM). Density Functional Theory (DFT) based calculations show that HOMO-LUMO band gap of HDT is altered after the conjugation and two-S binding (handle-like) configuration is energetically most favorable among three different structures. This study displays that the facile thiol functionalization process of MoS_2 is promising strategy for obtaining solution processable MoS_2.

1. Introduction

Modification of electronic, vibrational and optical properties of surfaces by organic molecule adsorption is one of the most efficient technique in nanoscale device fabrication. Organic molecule-functionalized materials have potential use in many applications such as molecular switches [1], sensors [2], photovoltaics [3], energy materials [4], lithography, [5] molecular recognition [6] and optoelectronics [7].

Organic and biological molecules provide an important tool for understanding of complex reactive functionalities and architectures at surface [8]. This is particularly true because in most cases, the organic layers provide a more sophisticated activity, passivation or selectivity function [9]. In addition, surfaces composed of complex molecules pave the way for investigation of single molecule levels [10] and identifying material properties that arise from functionalized surface with molecules [11]. Therefore, the use of organic adsorbates as a template for deposition on surface processes has the potential to obtain the surfaces in any form on mesoscopic and nanoscopic scales [12].

Two-dimensional transition metal dichalcogenides (TMDs) draw great interest due to their unique properties and their wide range of applications such as electronic devices [13], optoelectronics [14], biosensing, [15] catalysis [16]. Experimental researches in recent years have focused on the functionalization of such layered materials with molecules to contribute characteristics of TMDs materials. MoS_2 is a kind of TMDs and is used as an model system for functionalization steps [16].

MoS_2 is one of the most commonly TMDs due to its size-dependent optical and electronic properties. The MoS_2 crystal structure consists of 0.65 nm thick layers of Mo atoms coordinated between two sulfide planes, which are stacked and separated by a van der Waals gap [17]. MoS_2 is known to have a direct band gap of ~1.9 eV as a single MoS_2 layer and an indirect band gap of ~1.2 eV as a bulk MoS_2 crystal. Single-layer MoS_2 also has a good carrier mobility and a high current on/off ratio [18].

Moreover, the study of covalent functionalization of MoS_2 has been increased recently because functionalization of MoS_2 is a promising candidate for many applications and MoS_2 has been a pioneer for exploring materials having unique properties [19]. For example, conjugation of poly ethylene glycol (PEG) containing hydroxyl, carboxyl and trimethyl ammonium groups with MoS_2 provides stability in water [20]. Zhou *et al* reported that surface modification ofn-Butyllithium exfoliated MoS_2 with Mercaptopropionic acid (MPA), thioglycerol (TG) and cysteine which is aimed to alter physical properties of MoS_2 and obtain chemically reactive nanosheets. This makes the materials more versatile as a new candidate for producing functional layered MoS_2 for various applications [21].

Anbazhagan *et al* reported functionalization of bulk MoS_2 with thioglycolic acid (TGA) overnight, prior to sonication of the mixture in water and following dialysis is resulted in the binding of thiol caused delamination of the nanosheets with introduction of surface negative charge. Based on XRD results, the material which is 2H polytype semi-conductor with a bandgap is suitable for fluorescence studies. In this way, treatment of the TGA with MoS_2 opens the door to make stable non-heavy metal biomarkers [22].

Dravid *et al* expressed the reaction between MoS_2 and dodecanethiol to show selective bonding of thiol groups to the Mo atoms. This interaction is explained as ligand conjugation of MoS_2 which is described as arrangement of the thiol to Mo-atoms at sulfur vacancies by forming Mo-S bond [23].

MoS_2 shows generally the atomic ratio of Mo:S approximately 1.8:1 which is proved by x-ray Photoelectron Spectroscopy (XPS) [24]. The formation of Mo-S bond is due to fact that unsaturated Mo on the surface of MoS_2 is tendency for binding covalently to sulfur vacancy sites because the sulfur vacancies on the basal plane of MoS_2 act as catalytic reaction sites. Therefore, molecules having thiol group creates chemisorbed bonds with MoS_2 in the sulfur vacancy [25]. Makarova *et al* proved that adsorption of thiol molecules at sulfur vacancies on the basal plane of MoS_2 with scanning tunneling microscopy (STM).

Sulfur vacancies are important for the n-type characteristics of MoS_2, when it is used as a semiconductor device because the modification of thiol molecules on MoS_2 would be able to alter the electrical properties of MoS_2 by passivating sulfur vacancies of MoS_2 with thiol molecules [26].

With the combination of a well-known monolayer material, 2H-MoS_2, and another molecule known from the literature. We also show that monolayer 2H-MoS_2 can be functionalized with the HDT molecule for the first time.

In this study, a new material that results from the conjugation of HDT molecules with MoS_2 is investigated and characterized fro the first time. We theoretically and experimentally investigate structural, vibrational and electronic properties of conjugation of HDT on MoS_2 structure. The paper is organized as follows: computational and experimental methodology are given in details in sections 2 and 3, respectively. First principle calculation and experimental results are given in section 4. Finally we discuss the results in section 5.

2. Computational methodology

The structural and electronic properties of HDT-conjugated MoS_2 were investigated by using Vienna *ab initio* simulation package (VASP) [27–29]. In order to examine electron exchange and correlations, the generalized gradient approximation (GGA) in the Perdew-Burke-Ernzerhof PBE [30] was used. The van der Waals interaction was included by using DFT-D2 method of Grimme [31, 32]. The charge transfer between atoms was obtained by using Bader Technique [33]. The vibrational properties were also investigated using the small-displacement method implemented in PHON code [34].

The calculations were performed by using the following parameters. The energy cut-off for the plane wave basis set was taken to be 500 eV. As a convergence criterion for ionic relaxation, the total energy difference between the sequential steps in the iterations was taken 10^{-5} eV. The total Hellmann-Feynman forces on each unit cell was reduced to 10^{-4} eV/Å. In case of single molecule, we constructed a large supercell in which the vacuum is considered at least 10 Å in all directions in order to isolate the molecule. For single molecule on MoS_2, $4 \times 4 \times 1$ supercell of MoS_2 was considered to avoid interaction between the adjacent hexanedithiol molecules in the crystal $3 \times 3 \times 1$ Γ-centered *k*-point mesh was used as a Brillouin Zone sampling for large supercells.

The binding energy, E_b, was calculated with the following formula

$$E_b = E_{MoS_2} + E_{HDT} - E_{MoS_2+HDT} \quad (1)$$

where, E_{MoS_2} and E_{HDT} are the ground state energies of a monolayer MoS_2 and a single HDT molecule (without H atom(s) at the edge(s)), respectively. E_{MoS_2+HDT} represents the ground state energy of the HDT (without H atom(s) at the edge(s)) binded on the MoS_2 surface .

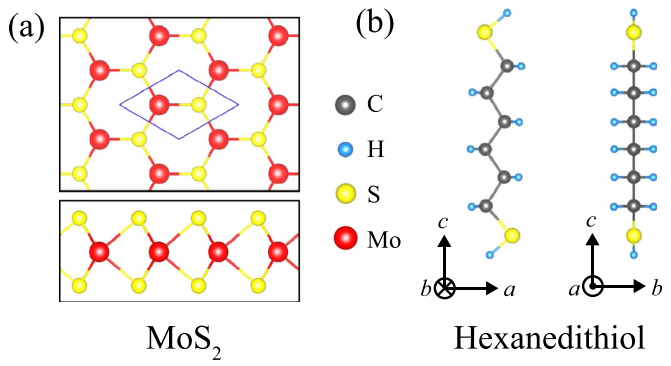

Figure 1. Calculated geometries of (a) single layer MoS_2 as top and side view and (b) HDT in two different in view of two different coordinate orientations.

3. Experimental methodology

3.1. Materials

Bulk MoS_2 crystal was purchased from 2dsemiconductors.com. Ethanol (% 99, Sigma-Aldrich), 1,6-Hexanedithiol (% 96, Sigma-Aldrich), Silicon (p-type; 100, Silicon Inc.) and SiO_2 (300 nm)/n-Si (University Wafer, USA) was used as received. DI water (18.2 M Ω cm^{-1}) treated through reverse osmosis (Thermo Scientific) was used. All chemicals were used as received.

3.2. Conjugation of Few-layer MoS_2 with 1,6-Hexanedithiol

MoS_2 samples were prepared by liquid exfoliation method. Few-layer MoS_2 were prepared by mixing in 2–3 ml solutions of the MoS_2 powder dissolved in ethanol/water (0.5 mg/ml-2 mg/ml). The MoS_2 suspensions were sonicated for 120 min at a power of 225 W in a water-cooled bath. After the sonication, The resultant raw dispersions were centrifuged at 12000 rpm for 30 min. The top 3/4 of the supernatant was decanted and used for conjugation. The sediment was discarded or reused for further exfoliation. HDT was prepared in ethanol at the appropriate concentration. MoS_2 solution and HDT molecule were mixed for an hour and incubated overnight. The thicknesses of MoS_2 flakes are similar as given in our previous study [35].

4. Results and discussion

4.1. Characteristic properties of 1,6-Hexanedithiol and MoS_2 crystal

4.1.1. Structural properties

A layer of MoS_2 is composed of three hexagonally packed trigonal atomic sublayers. The sublayer of Mo atoms are sandwiched between two sublayers of S atoms in 2H phase with the stacking corresponding to the order of ABA as shown in figure 1(a). The lattice constant of single-layer MoS_2 is found to be 3.19 Å and the Mo-S bond length is 2.41 Å. S_b-Mo-S_u angle is 80.5° and the distance between S_b and S_u is 3.12 Å (the subscripts, *b* and *u*, are bottom and up, respectively). The charge donation of a Mo atom to each S atom is ∼0.6 *e* indicating covalent type bonding between Mo and S atoms. Individual MoS_2 layers are stacked by the weak vdW-type interaction in its few-layer or bulk forms. The lamellar structure of MoS_2 provides clean surfaces which is suitable for the covalent functionalization by thiol group [23, 36, 37].

The HDT molecule consists of 6 C atoms in zig-zag chain-like structure in which each C atom is arranged in two H atoms and also by S atoms at the edges of molecule. Thus, each C atom constructs tetrahedral bond configuration. Edge S atoms are also saturated by the single H atom as shown in figure 1(b). The C-C, C-H, S-C, and S-H bond lengths are found to be 1.53, 1.10, 1.83, and 1.35 Å, respectively. The overall shape of the hexanedithiol is straight with the length of ∼11.0 Å.

4.1.2. Vibrational properties

In figures 2(a) and (b), the phonon band structure and Raman measurement are given, respectively. Firstly, the calculated phonon band structure (see figure 2(a)) exhibits 3 acoustic and 15 optical modes. Due to degeneracies of the modes, 8 different non-zero frequency levels appear at Γ point. Secondly, as given in figure 2(b), the Raman spectrum has 4 prominent peaks at ∼200, ∼380, ∼405 and ∼460 cm^{-1}. Except the peak at ∼200 cm^{-1}, the peaks correspond to well known Raman active modes of the bulk MoS_2 and the spectrum confirms the literature.

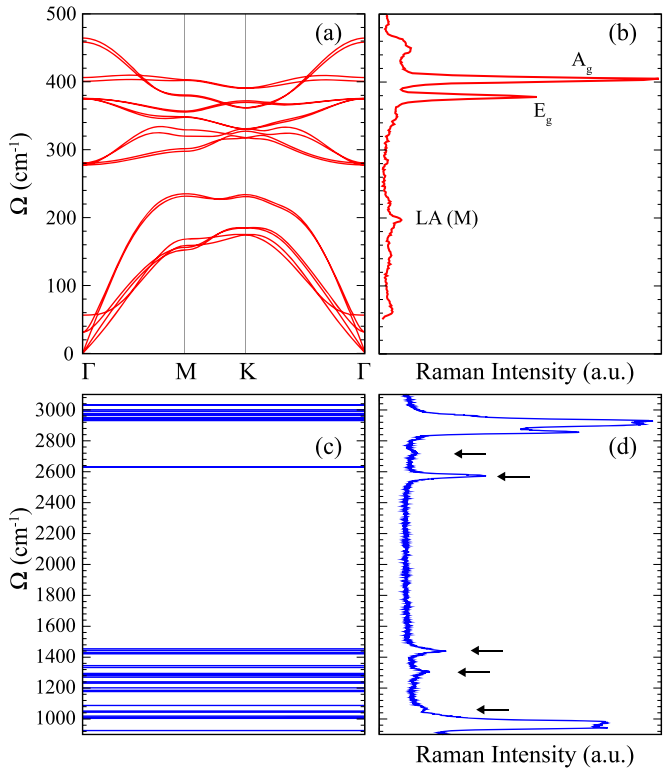

Figure 2. (a) Phonon band structure of bulk MoS_2 (b) Raman spectrum of bulk MoS_2. (c) The phonon modes of the HDT molecule. (d) Raman spectrum of the HDT molecule.

The comparison of the calculated phonon band structure and Raman spectrum shows that the frequencies of the modes at the Γ point perfectly match with the frequencies of the peaks at the Raman spectrum. On the other hand, the peak at ~200 cm^{-1} is known to be disorder-induced first order of LA(*M*) phonons as shown in figure 2(b) [38]. Raman spectrum shows that we have few-layer defected MoS_2 layer.

The phonon modes and Raman spectrum of the HDT molecule are also given in figures 2(c) and (d), respectively. The characteristic phonon modes as flat lines and the peaks in the Raman spectrum are marked by black arrows. It is clearly seen that the phonon modes and peaks in the Raman spectrum match except for the highest level having a slight shift from the peak at ~2560 cm^{-1}. The good accord between the calculated Phonon bands and measured Raman spectra enables us that examine the characteristic phonon levels and the Raman peaks.

4.1.3. Electronic properties

We also investigate the electronic properties of MoS_2 and HDT structures as shown in figure 3. It is known that MoS_2 is a semiconductor with an indirect band gap in its bulk form and direct band gap in the single-layer form [39]. Here, we consider the single layer of MoS_2 and a direct band gap is found to be 1.54 eV with GGA. In order to predict the band alignment between MoS_2 and HDT, the work function of MoS_2 is also calculated to be 5.7 eV. It should be noted that the work function values of bulk, few-layer and single-layer MoS_2 are similar due to very low interlayer interaction.

On the other hand, as given in figure 3(a), the energy difference between HOMO and LUMO levels of the HDT is calculated to be 4.32 eV which is significantly high as compared to band gap of MoS_2. In figure 3(b), the partial charge densities of the HOMO and LUMO levels of HDT are given. The main difference between the HOMO and LUMO charge densities is that, considering the plane of C zig-zag chain, the partial charge density of the HOMO level seems out-of-plane *p*-like orbital of the S atoms and the partial charge density of the LUMO level resembles in-plane *p*-like orbitals. The work function of the HDT is found to be 5.3 eV which is 0.4 eV higher that that of MoS_2.

As given in figure 3(a), the energy band diagram of single-layer MoS_2 and the molecular energy levels of HDT are aligned with respect to work functions and thus the band alignment of the HDT-conjugated MoS_2 is predicted to be Type II where valence band maximum (VBM) and conduction band minumum (CBM) originate from HDT and MoS_2, respectively. This situation would be valid, if the interaction between the HDT molecule

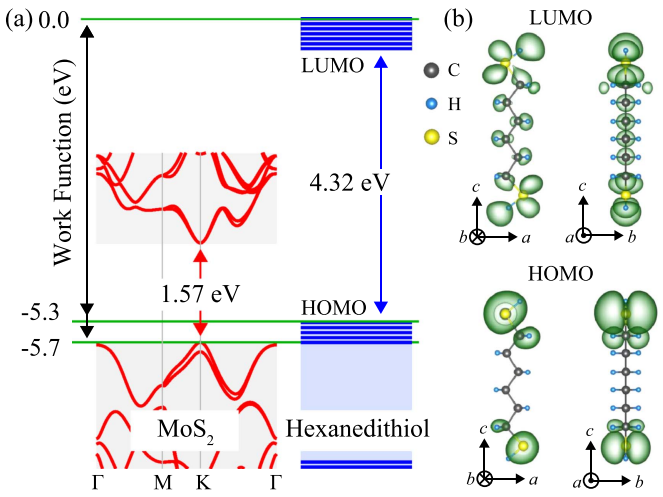

Figure 3. (a) The calculated electronic band structure and decomposed charge densities of single layer MoS_2 and molecular energy levels of HDT are aligned with respect to vacuum levels and the work functions. (b) The partial charge densities of the HOMO and LUMO states are shown two different view angle. Color code of the atoms and the coordinate orientations for the molecule are given.

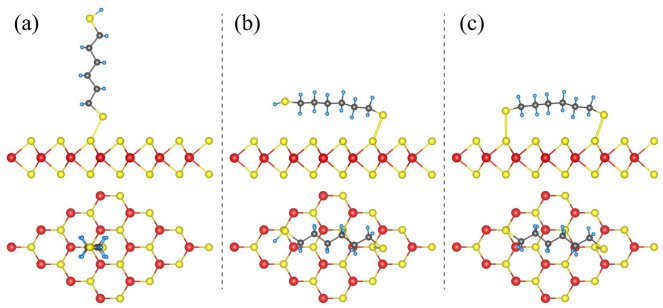

Figure 4. Structural configurations of HDT molecule on MoS_2. (a) Standing, (b) lying with one-S binding, and (c) two-S binding (handle-like) are shown.

and MoS_2 surface does not alter the band dispersions and the band alignment. In the following sections, the HDT-conjugated MoS_2 is discussed.

4.2. Conjugation of 1,6-Hexanedithiol on MoS_2

4.2.1. Structural properties

In order to investigate the structure of HDT-conjugated MoS_2, we consider three different structural configurations; standing of the molecule over the MoS_2 surface and two lying configurations as shown in figure 4. Our calculations show that the hexanedithiol binds to the MoS_2 surface in three different cases. In the standing one, the hexanedithiol is in perpendicular configuration and the length of S-S bond between MoS_2 and HDT molecule is 2.52 Å. In one of the lying configurations as shown in figure 4(b), the hexanedithiol binds to the MoS_2 surface by its single S atom and the other S atom of the molecule is terminated by a single H and the S-S bond length is found to be 2.62 Å. The other lying configuration is a handle-like structure as shown in figure 4(c) in which S atoms at edges of hexanedithiol bind to MoS_2 surface with S-S bond lengths of 2.58 and 2.81 Å. In both cases, the molecules are slightly banded over the surface. The binding energies of the standing, one-S binding and two-S binding structures are found to be 0.22, 0.76, and 0.86 eV, respectively, which means that two-S binding (handle-like) configuration is the energetically most favorable one.

Although, the standing configuration has the minimum S-S bond length as compared to laying configurations, it has the minimum binding energy which indicates that not only the S-S interaction but also the interaction between the main part of the HDT and surface of MoS_2 contributes and increases the binding energy of the molecule.

Figure 5 shows SEM images of bulk MoS_2 and HDT-conjugated MoS_2. According to figure 5(a), the size of MoS_2 flakes vary between 0.25 and 1.25 μm. The conjugation of the MoS_2 flakes by hexanedithiol are presented

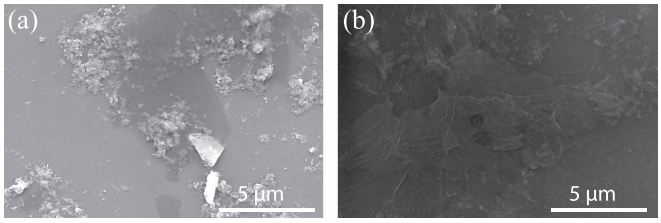

Figure 5. SEM images of Bulk MoS_2 (a) and (b) HDT-conjugated MoS_2.

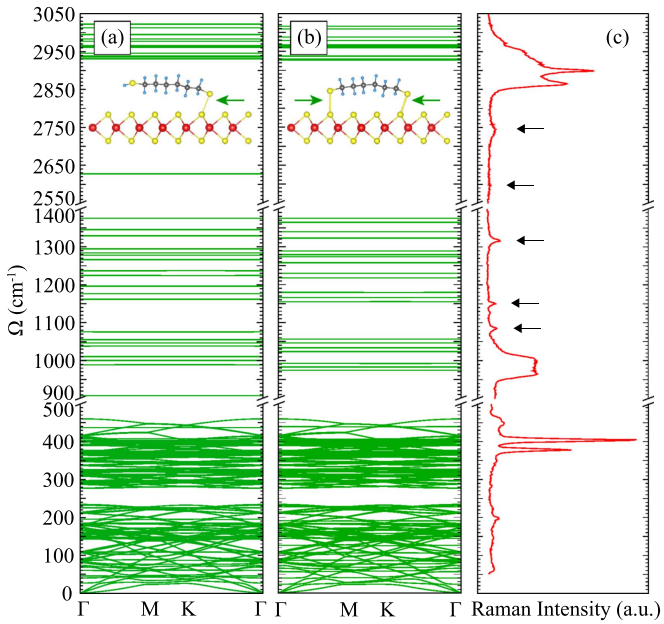

Figure 6. Phonon band structures of HDT-conjugated MoS_2 for (a) one-S and (b) two-S structures. (c) Raman spectrum is aligned to the phonon band structures with respect to frequency axis. The small peaks in the Raman spectrum are marked by black arrows.

in figure 5(b). Due to small size of the hexanedithiol molecules, the SEM images of both MoS_2 and HDT-conjugated MoS_2 exhibit nearly similar structures.

4.2.2. Vibrational properties

The vibrational properties of HDT-conjugated MoS_2 also investigated. In figure 6, the phonon band structures of one-S and two-S binding of HDT on MoS_2 (see in figure 4) are shown and compared with the Raman intensity measurement. First of all, in the lower part of the phonon band structures (0–500 cm^{-1}) in figures 6(a) and (b), the most of the bands have dispersion over the considered path on the Brillouin Zone indicating that these modes originate from MoS_2. As shown in figure 6(c) for the same frequency region, the Raman measurement demonstrates two characteristic peaks of the MoS_2 as expected, and there is no prominent peak under the MoS_2 peaks.

Secondly, in the frequency region of 900 and 1400 cm^{-1}, the phonon bands are totally flat which indicates the vibrational states belong to HDT. In addition, in the Raman spectrum at 900–1400 cm^{-1}, there are well-known peaks of the HDT which have small intensities as compared to those of MoS_2. Two Raman peaks at ~1085 and ~1150 cm^{-1} represent the C-C stretching [38]. These modes reveal important information concerning the conformational order of the aliphatic chain in dithiols [40].

For higher frequencies (2550–3050 cm^{-1}), the phonon bands correspond to C-H and S-H stretching modes, respectively. The phonon bands are compatible with Raman spectra. The significant peak in the Raman spectrum is observed at ~2560 cm^{-1} for HDT-conjugated MoS_2. This peak originates from S-H stretching mode and while the one-S binding structure has corresponding phonon band at the phonon band structure in figure 6(a), the two-S binding case does not have the phonon band at that level. It appears that most of the HDT loss S-H bonds then HDT binds to the MoS_2.

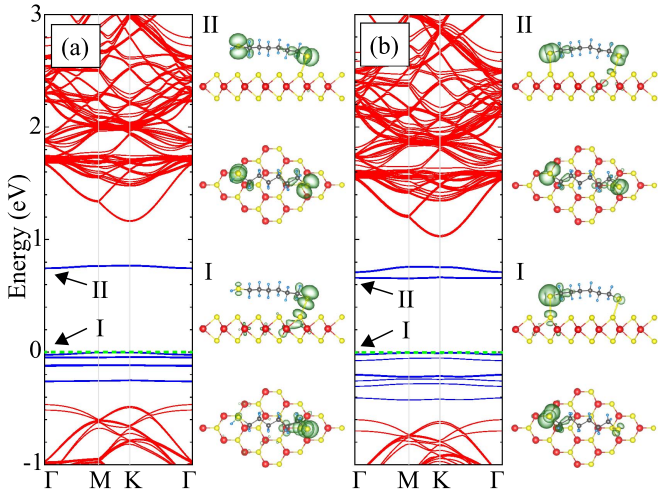

Figure 7. Electronic band structures of (a) one-S and (b) two-S binding of the hexanedithiol on MoS_2. Flat bands at the top of VB and bottom of the CB are referred by black arrows and the top and side views of corresponding partial charge densities are shown at the right side of the electronic band structures.

Also, another indication of binding of HDT on MoS_2 is that characteristic peaks of HDT are found between ~2860 and ~2930 cm^{-1} which correspond to the C-H stretching modes. The Raman peak at ~2860 cm^{-1} is attributed to an overtone of CH_2 bending in Fermi resonance with CH_2 vibration, while the latter band is attributed to CH_2 [41]. The other Raman peak of ~2903 cm^{-1} is assigned to the CH_2 vibration [42]. Therefore, we can deduce that the two-S binding configuration exists on the MoS_2 surface more than one-S binding case. Our results show that MoS_2 is covalently conjugated by the HDT molecules.

4.2.3. Electronic Properties

We also investigate the electronic properties of HDT-conjugated MoS_2. The energy band structure of two different binding configurations are shown in figures 7(a) and (b) which correspond to one-S and two-S binding cases, respectively. Due to having lower binding energy, we do not focus on the standing configurations. Both systems have almost flat occupied bands at the vicinity of the Fermi-level indicating that these localized states originate from the HDT molecule. There are also unoccupied flat bands which appeare as midgap states after conjugation of HDT.

The minimum energy difference between the occupied and unoccupied flat bands are found to be 0.76 and 0.65 eV for one-S and two-S binding cases, respectively. The partial charge density of the highest occupied band, labeled by I, resembles the HOMO level of the individual hexanedithiol molecules with hybridizations to the underlying S and Mo atoms. The midgap flat band, on the other hand, arises from S atoms of the HDT molecule as shown in panels II of figures 7(a) and (b) and resembles the LUMO level of the individual hexanedithiol. It seems that covalent interaction between the HDT and MoS_2 reduces the LUMO level of the HDT and it appears as a midgap state. The bands having energy dispersion over the *k*-space are originated from MoS_2 crystal. According to these states, the system has indirect band gap of 1.62 eV for both one-S and two-S binding cases. All in all, the theoretical investigation shows that the hexanedithiol covers the MoS_2 surface and MoS_2 is conjugated electronically.

5. Conclusions

In this study, structural, vibrational and electronic properties of HDT-conjugated MoS_2 were investigated via Raman spectroscopy and DFT-based calculations. Raman spectroscopy analysis revealed that after the conjugation process, the most of the HDT molecules bind to MoS_2 surface in two-S binding configuration that is the most favorable configuration as compared to standing and lying configurations of the one-S binding. DFT results indicate that the HOMO-LUMO band gap of HDT is calculated and it is modified after the conjugation. The MoS_2/HDT system has type I band alignments where the VBM and CBM originate from the localized HDT states in terms of two-s binding. The midgap flat band arises from S atoms of the HDT molecule. To sum up, presence of functional groups on MoS_2 make easier for attachment of molecules and nanoparticles to meet specific demands.

Acknowledgments

Computational resources were provided by TUBITAK ULAKBIM, High Performance and Grid Computing Center (TR-Grid e-Infrastructure). HS acknowledges financial support from the TUBITAK under the project number 116C073. HS acknowledges support from Bilim Akademisi-The Science Academy, Turkey under the BAGEP program.

ORCID iDs

A Gul https://orcid.org/0000-0001-5386-7749
B Akbali https://orcid.org/0000-0002-6852-2193

References

[1] Tautz F S 2007 Structure and bonding of large aromatic molecules on noble metal surfaces: the example of PTCDA *Prog. Surf. Sci.* **82** 479–520
[2] Lu W and Lieber C M 2007 Nanoelectronics from the bottom up *Nat Mater* **6** 841–50
[3] Waser R and Aono M 2007 Nanoionics-based resistive switching memories *Nat Mater* **6** 833–40
[4] Koch N *et al* 2008 Adsorption-induced intramolecular dipole: correlating molecular conformation and interface electronic structure *J. Am. Chem. Soc.* **130** 7300–4
[5] Morgenstern K 2011 Switching individual molecules by light and electrons: from isomerisation to chirality flip *Prog. Surf. Sci.* **86** 115–61
[6] Kuhnle A, Linderoth T R, Hammer B and Besenbacher F 2002 Chiral recognition in dimerization of adsorbed cysteine observed by scanning tunnelling microscopy *Nature* **415** 891–3
[7] Xu H, Chen R, Sun Q, Lai W, Su Q, Huang W and Liu X 2014 Recent progress in metal-organic complexes for optoelectronic applications *Chem. Soc. Rev.* **43** 3259–302
[8] Barlow S M and Raval R 2003 Complex organic molecules at metal surfaces: bonding, organisation and chirality *Surf. Sci. Rep.* **50** 201–341
[9] Netzer F P and Ramsey M G 1992 Structure and orientation of organic molecules on metal surfaces *Crit. Rev. Solid State Mater* **17** 397–475
[10] Tkatchenko A, Romaner L, Hofmann O T, Zojer E, Ambrosch-Draxl C and Scheffler M 2011 Van der Waals interactions between organic adsorbates and at organic/inorganic interfaces *MRS Bull* **35** 435–42
[11] Nazin G V, Qiu X H and Ho W 2003 Visualization and spectroscopy of a metal-molecule-metal bridge *Science* **302** 7781
[12] Schon J H, Meng H and Bao Z 2001 Self-assembled monolayer organic field-effect transistors *Nature* **413** 713–6
[13] Zhang H, Loh K P, Sow C H, Gu H, Su X, Huang C and Chen Z K 2004 Surface modification studies of edge-oriented molybdenum sulfide nanosheets *Langmuir* **20** 6914–20
[14] Nicolosi V, Chhowalla M, Kanatzidis M G, Strano M S and Coleman J N 2013 Liquid exfoliation of layered materials *Science* **340** 1226419
[15] Chhowalla M, Shin H S, Eda G, Li L-J, Loh K P and Zhang H 2013 The chemistry of two-dimensional layered transition metal dichalcogenide nanosheets *Nat. Chem.* **5** 263–75
[16] Zeng Z, Yin Z, Huang X, Li H, He Q, Lu G, Boey F and Zhang H 2011 Single-layer semiconducting nanosheets: high-yield preparation and device fabrication *Angew. Chem. Int. Ed* **50** 11093–7
[17] Ganatra R and Zhang Q 2014 Few-layer MoS_2: a promising layered semiconductor *ACS Nano* **8** 4074–99
[18] Jariwala D, Sangwan V K, Lauhon L J, Marks T J and Hersam M C 2014 Emerging device applications for semiconducting two-deimensional transition metal dichalcogenides *ACS Nano* **8** 1102–20
[19] Presolski S and Pumera M 2016 Covalent functionalization of MoS_2 *Mater. Today* **19** 140–5
[20] Liu T, Wang C, Gu X, Gong H, Cheng L, Shi X, Feng L, Sun B and Liu Z 2014 Drug delivery with PEGylated MoS_2 nano-sheets for combined photothermal and chemotherapy of cancer *Adv. Mater* **26** 3433–40
[21] Zhou L, He B, Yang Y and He Y 2014 Facile approach to surface functionalized MoS_2 nanosheets *RSC Adv* **4** 32570–8
[22] Anbazhagan R, Wang H J, Tsai H C and Jeng R J 2014 Highly concentrated MoS_2 nanosheets in water achieved by thioglycolic acid as stabilizer and used as biomarkers *RSC Adv* **4** 42936–41
[23] Chou S S, Deas M, Kim J, Byun S, Dykstra C, Yu J, Huang J and Dravid V P 2013 Ligand conjugation of chemically exfoliated MoS_2 *J. Am. Chem. Soc* **135** 4584–7
[24] Backes C, Berner N C, Chen X, Lafargue P, LaPlace P, Freeley M, Duesberg G S, Coleman J N and McDonald A R 2015 Functionalization of liquid-exfoliated two-dimensional 2H- MoS_2 *Angewandte Chemie International Edition* **54** 2638–42
[25] Cho K *et al* 2015 Electrical and optical characterization of MoS_2 with sulfur vacancy passivation by treatment with alkanethiol molecules *ACS Nano* **9** 8044–53
[26] Makarova M, Okawa Y and Aono M 2012 Selective adsorption of thiol molecules at sulfur vacancies on MoS_2(0001), followed by vacancy repair via S-C dissociation *J. Phys. Chem.* C **116** 22411–6
[27] Kresse G and Hafner J 1993 *Ab initio Phys. Rev.* B **47** 558–61
[28] Kresse G and Furthmller J 1996 *Phys. Rev.* B **54** 11169
[29] Kresse G and Joubert D 1758 *Phys. Rev.* B **59** 1999
[30] Perdew J P, Burke K and Ernzerhof M 1996 Generalized gradient approximation made simple *Phys. Rev. Lett.* **77** 3865–8
[31] Grimme S 2006 Semiempirical GGA-type density functional constructed with a long-range dispersion correction *J. Comput. Chem.* **27** 1787–99
[32] Bucko T, Hafner J, Lebègue S and Ángyán J G 2010 Improved description of the structure of molecular and layered crystals: *Ab initio* DFT calculations with van der Waals corrections *J. Phys. Chem.* A **114** 11814–24
[33] Bader R F W 1990 *Atoms in Molecules—A Quantum Theory* (Oxford, UK: Oxford University Press)
[34] Alfe D 2009 PHON: a program to calculate phonons using the small displacement method *Comp. Phys. Commun* **180** 2622–33

[35] Akbali B, Yanilmaz A, Tomak A, Tongay S, Çelebi C and Sahin H 2017 Few-layer MoS_2 as nitrogen protective barrier *Nanotechnology* **28** 415706415706–14
[36] Divigalpitiya W M R, Frindt R F and Morrison S R 1989 Inclusion systems of organic molecules in restacked single-layer molybdenum disulfide *Science* **246** 369–71
[37] Raybaud P, Hafner J, Kresse G and Toulhoat H 1998 Adsorption of thiophene on the catalytically active surface of MoS_2: an *ab initio* local-density-functional study *Phys. Rev. Lett.* **80** 1481–4
[38] Frey G L, Tenne R, Matthews M J, Dresselhaus M S and Dresselhaus G 1999 Raman and resonance Raman investigation of MoS_2 nanoparticles *Phys. Rev.* B **60** 2883–92
[39] Mak K F, Lee C, Hone J, Shan J and Heinz T F 2010 Atomically thin MoS_2: a new direct-gap semiconductor *Phys. Rev. Lett.* **105** 136805
[40] Chakraborty B, Matte H S S R, Sood A K and Rao C N R 2013 Layer-dependent resonant Raman scattering of a few layer MoS_2 *J. Raman Spectrosc* **44** 92–6
[41] Abbate S, Zerbi G and Wunder S L 1982 Fermi resonances and vibrational spectra of crystalline and amorphous polyethylene chains *J. Phys. Chem.* **86** 3140–9
[42] Koroteev V O, Bulusheva L G, Okotrub A V, Yudanov N F and Vyalikh D V 2011 Formation of MoS_2 nanoparticles on the surface of reduced graphite oxide *Phys. Status Solidi* B **248** 2740–3